

Liquid gallium in confined droplets under high-temperature and high-pressure conditions

R. Poloni and S. De Panfilis

European Synchrotron Radiation Facility, B.P. 220, F-38043 Grenoble, France

A. Di Cicco

*Istituto Nazionale per la Fisica della Materia (INFM) and Dipartimento di Fisica, Università degli Studi di Camerino,**Via Madonna delle Carceri, I-62032 Camerino (MC), Italy**and Istituto Nazionale di Fisica Nucleare (INFN), Laboratori Nazionali di Frascati, Via E. Fermi, 40, I-00044 Frascati (Roma) Italy*

G. Pratesi, E. Principi, and A. Trapananti

*Istituto Nazionale di Fisica della Materia, and Dipartimento di Fisica, Università di Camerino, Via Madonna delle Carceri,**62032 Camerino (MC), Italy*

A. Filipponi

Dipartimento di Fisica, Università dell'Aquila, Via Vetoio, 67010 Coppito, Italy

(Received 1 October 2004; revised manuscript received 24 January 2005; published 27 May 2005)

Phase transitions and the local structure of micrometric droplets of liquid gallium under pressure were studied by combining extended x-ray absorption fine structure, single-energy x-ray absorption detection (SEXAD), and energy-scanning x-ray diffraction (ESXD). Measurements were performed in a range of pressures and temperatures of 0–6.7 GPa and 298–440 K, respectively. The samples for the high-pressure measurements were obtained by using an emulsion of gallium into epoxy resin, a procedure previously developed by the authors. The distribution of droplets was fully characterized by scanning electron microscopy. We found that the liquid can be kept in a metastable state well beyond the liquid-solid coexistence line (1.9 GPa at 300 K). Considering both the ESXD patterns and the SEXAD scans, we infer that the quantity of crystallized gallium droplets increases as a function of pressure, while no sign of crystallization is observed up to 2.7 GPa. The structural and crystallization properties of Ga emulsions, including the determination of the short-range radial distribution function, were measured by XAS in an extended range of pressures and temperatures, putting to a test the possible existence of different Ga-liquid polymorphs.

DOI: 10.1103/PhysRevB.71.184111

PACS number(s): 61.10.Ht, 61.25.Mv, 64.60.My, 62.50.+p

I. INTRODUCTION

Gallium is a low-melting-point metal ($T_m=302.9$ K) with an *ice-type* phase diagram that displays an extended polymorphism with several phase transitions and metastable modifications as a function of pressure and temperature. The density of the liquid phase at ambient pressure exceeds by about 3% that of the stable crystalline phase. This metal in the liquid state can be also subject to a deep undercooling. Pioneering studies on the undercooling properties of liquid metals were performed by Turnbull and coworkers,^{1–3} showing that the solidification temperatures could be depressed in isolated droplets up to 0.13–0.33 times the absolute melting temperature. For Ga droplets, in particular, deep undercooling limits up to $\Delta T/T_m \approx 0.325$ (Ref. 4) were obtained, and evidence for deep undercooling $\Delta T/T_m \approx 0.5$ was found by using inelastic neutron-diffraction measurements.⁵ These findings are in agreement with the results of the molecular-dynamics simulation.⁶ More recently, extended x-ray absorption fine structure (EXAFS) and EDXD measurements confirmed this scenario;⁷ the maximum undercooling observed for a confined Ga fluid was about 150 K, while the melting point was depressed down to 245 K.

An additional interest in this system stems from the possible existence of liquid-liquid phase transitions in the high-pressure, undercooled liquid domain. The theoretical expla-

nations for the occurrence of liquid-liquid phase transitions are often based on the assumption of a complex potential.^{8–10} This occurrence raises interest in elements such as Sn, Bi, Ga, and Sb, which are characterized by the coexistence of metallic and covalent characters, causing a distortion in the local structure.

The aim of this paper is to investigate the local structure of gallium in its stable and metastable liquid phase as a function of pressure, using advanced techniques¹¹ with a sufficient sensitivity to small structural modifications. Samples consisting of a dispersion of micrometric gallium droplets in an inert rigid matrix have been shown to exhibit undercooling capabilities.^{7,12,13} In this paper we present measurements of emulsions of micrometric droplets of liquid gallium under pressure, combining extended x-ray absorption fine structure (EXAFS), single-energy x-ray absorption detection (SEXAD), and energy-scanning x-ray diffraction (ESXD). These advanced techniques are in fact expected to shed light on possible structural modifications induced in liquid gallium by the application of an external pressure.

II. EXPERIMENTAL DETAILS

Ga *K*-edge x-ray absorption spectroscopy (XAS) measurements and ESXD patterns were collected at the European

Synchrotron Radiation Facility (ESRF) on the bending-magnet beam line BM29.¹⁴ Accurate EXAFS experiments were performed using a high-stability fixed-exit double-crystal Si(311) monochromator, achieving an excellent resolution better than $\Delta E/E \approx 5 \times 10^{-5}$ with 0.25-mm primary vertical slits at 23.5 m from the source at the Ga *K* edge. ESXD patterns, as a function of pressure, were recorded with a transmission geometry setup consisting of a multichannel collimator¹⁵ of seven detectors (CdZnTe) placed at fixed angles 2θ .

The full width at half maximum (FWHM) of the Bragg peaks corresponds to a $\Delta\theta/\theta$ in the 10^{-3} range. The improvement of the powder statistic was achieved by performing a sample oscillation of total amplitude $\Delta\omega = 4^\circ$ around the axis, orthogonal to the scattering plane.

The XAS spectra covered the 0–5.8 GPa pressure range and the 298–410 K temperature range. The V5 Paris-Edinburgh press¹⁶ was used as a pressure device, while temperature was monitored by a thermocouple placed into the gasket with an estimated uncertainty of 5 K.

The ESXD data were also used to obtain *in situ* pressure measurements monitoring changes in the *d*-lattice spacing of a pressure marker (LiF). The pressure was estimated using a Vinet equation of state (EOS),^{17,18}

$$P = 3B_0x^{-2}(1-x)\exp[\eta(1-x)] + \alpha_0B_0(T - T_R), \quad (1)$$

with a typical 0.1 GPa error bar coming from the uncertainty of the position of the Bragg peaks. In Eq. (1), $x = (V/V_0)^{1/3}$, B_0 is the equilibrium volume V_0 isothermal, bulk modulus [$B_0 = -VdP/dV$] and $\eta = (3/2)(\partial B_0/\partial P - 1)$. The knowledge of zero-pressure properties, V_0 , B_0 and the thermal expansion coefficient α_0 , at the reference temperature T_R (room temperature), is required. The values of $B_0 = 66.51$ GPa and $\eta = 6.45$ used in our calculation have been derived from ultrasonic measurements.^{19–22}

III. SAMPLE PREPARATION AND CHARACTERIZATION

The sample emulsions were prepared by mixing small quantities ($\sim 4\%$ in wt) of high-purity gallium (99.999%, Sigma-Aldrich) with the pressure marker (LiF) and epoxy resin above a temperature of 315 K. Gallium droplets were gradually broken into smaller droplets by the pressure of glass tools on a flat glass surface. The mixing procedure was stopped when the emulsion appeared macroscopically homogeneous and the hardener component was finally added to the mixture. We prepared several samples by using different kinds of epoxy resin. A good sample in order to prepare the final shape for the 7-mm gasket was obtained with 2ton epoxy resin (Devcon). This epoxy resin has a working time of 30 min and it completely solidifies 8 h after mixing it with the hardener. The limiting temperature, above which the compound *resin+hardener* decomposes is 350 K at ambient pressure, and it increases up to 463 K and 3.2 GPa. At higher pressures, the diffraction data have been collected up to a limiting temperature of about 400 K, and no sign of decomposition or contamination of Ga has been observed. Two different samples were prepared with this epoxy resin, sample A and sample B,

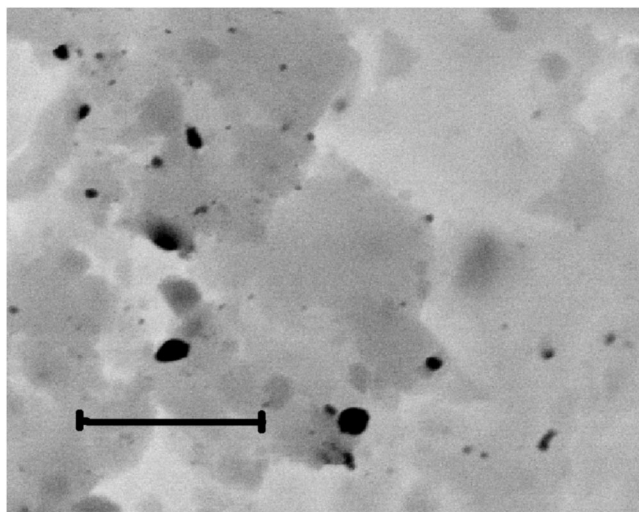


FIG. 1. SEM image in inverted luminosity of the surface of the gallium emulsion (sample *B*). The black spots are gallium droplets while the gray background is the epoxy resin. The horizontal bar corresponds to a $5\text{-}\mu\text{m}$ length.

with initial weight dilutions of Ga:Epoxy:Hardener:LiF = 1 : 10 : 10 : 1 and Ga:Epoxy:Hardener:LiF = 1 : 10 : 10 : 6, respectively.

The characterization of sample *B* was carried out by studying the droplet-size distribution using scanning electron microscopy. A graphite layer was deposited on the sample in order to obtain a conductive surface. In Fig. 1 we report a typical scanning-electron-microscopy (SEM) image in the inverted luminosity of a *B* gallium emulsion. The gray background is the epoxy resin, while the black spots are gallium droplets, and they were identified by fluorescence microanalysis.

Statistical analyses of the droplet-size distribution were carried out on a set of 38 pictures for a total of 597 droplets.

In Fig. 2 we report the histogram of the experimental droplet-diameter distribution δ of sample *B* and also the distribution of the logarithm of diameter λ . It is clear from the figure that our statistical analysis confirms previous

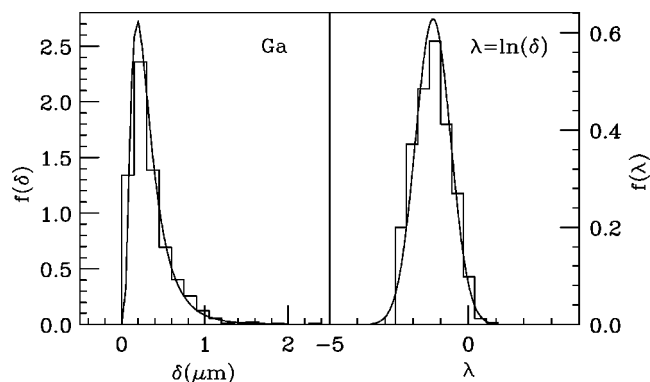


FIG. 2. Left panel: histogram of the gallium-droplet diameter δ determined from SEM image analysis and $f(\delta)$ probability density. Right panel: histogram of the logarithm λ of droplet diameters. The probability density $f(\lambda)$ as a function of λ is a Gaussian of the parameters $\bar{\lambda}$ and σ_λ^2 estimated from the statistical analysis.

results^{7,12,13} obtained for gallium emulsions. These works show that a log-normal model can reproduce the actual-size distribution in these emulsions. Moreover, the typical droplet size of our sample is well below 1 μm , as it was found in such works. Consequently, we expect our sample to have similar undercooling properties as those shown in Ref. 7 (i.e., undercooling down to 150 K and melting depressed down to 254 K). This means that at room temperature and ambient pressure our sample should be in the liquid phase. The comparison of the XAS spectrum of liquid gallium at 304 K and the ambient pressure in Ref. 7 and that of sample *B* confirmed that our emulsion at room-temperature and ambient-pressure conditions consists of liquid-gallium droplets.

The log-normal function distribution is defined as

$$f(\delta) = \frac{1}{\delta(2\pi\sigma_\lambda^2)^{1/2}} \exp\left[-\frac{(\ln \delta - \bar{\lambda})^2}{2\sigma_\lambda^2}\right]. \quad (2)$$

The probability density $f(\lambda)$ as a function of λ reported in Fig. 2 is given by a Gaussian of parameters $\bar{\lambda}$ and σ_λ^2 estimated from the statistical analysis. This curve is in good agreement with the distribution of the logarithm of the diameters.

The emulsions *A* and *B* were used to prepare suitable samples for XAS and ESXD measurements under high-pressure conditions.

The final emulsion shape was designed to fit the typical sample assembly of the ‘‘Paris-Edinburgh’’ large-volume press. In particular the emulsion was poured using a spatula and a needle into a 2-mm graphite, hollow cylinder in a 7-mm boron-epoxy gasket.¹⁶

IV. EXPERIMENTS

Two separate experiments were performed using the samples described in Sec. III. Extended x-ray absorption fine structure (EXAFS), single-energy x-ray absorption detection (SEXAD), and energy-scanning x-ray diffraction (ESXD) patterns were collected in a 0–6.7-GPa pressure range and a 298–410-K temperature range. Sample *A* resulted with a Ga *K*-edge absorption discontinuity of about 1.6 and was better suited to collect ESXD patterns at room temperature as a function of pressure. Sample *B*, with an absorption discontinuity at the Ga *K* edge of about 0.7, suitable to obtain low-noise, experimental XAS spectra, was instead used to collect EXAFS and SEXAD measurements. In this sample ESXD patterns were collected in a short-energy range only for pressure calibration.

In Fig. 3 we illustrate the ensemble of measurements taken on the two samples relative to the Ga phase diagram determined by previous works. The black lines (in the 0–7.5 GPa pressure range up to 423 K) correspond to the differential thermal analysis (DTA) measurements carried out by Jayaraman *et al.* in 1963.²³ They show the liquid-solid *l*- α Ga, *l*-Ga(II) and *l*-Ga(III) coexistence lines and the solid-solid α Ga-Ga(II), Ga(II)-Ga(III) phase transitions. The light lines in the 0–3.5-GPa pressure range and 233–333-K temperature range correspond to the phase diagram recon-

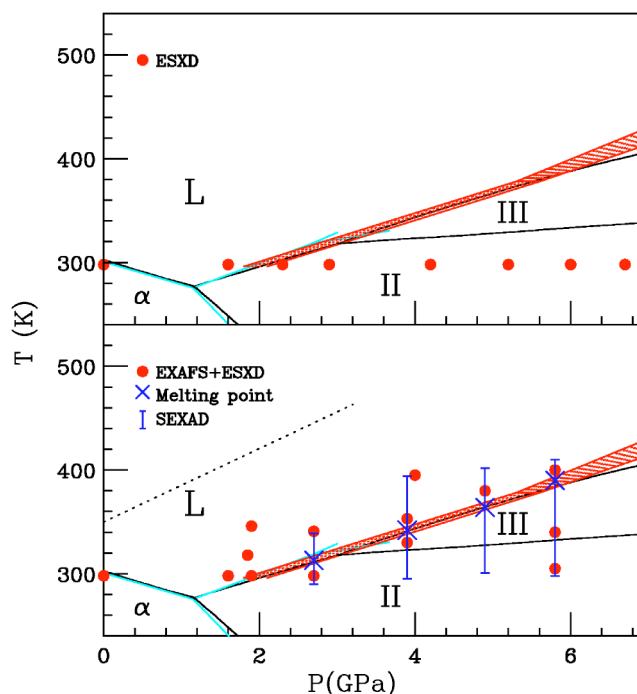


FIG. 3. Ga phase diagram and experimental points analyzed. Upper panel: ESXD measurements on sample *A*. Lower panel: EXAFS and ESXD measurements on sample *B*. In this experiment the ESXD patterns were collected in a short-energy range only for pressure calibration. The vertical bars correspond to the temperature range investigated during the SEXAD. We also report the melting points estimated from the *T*-scan analysis. The dotted line in the lower panel corresponds to the region below which the compound resin+hardener was not found to decompose.

structed by Bosio.²⁴ The high-pressure part of the phase diagram (up to 15 GPa at room temperature) was analyzed by Schulte and Holzappel.²⁵ More recently, the extension of Ga phase diagram up to 498 K and 29.8 GPa was carried out by using EDXD and EXAFS dispersive techniques.²⁶ The dashed oblique lines in the figure indicate the uncertainty in the liquid-Ga(III) phase transition.

V. ESXD RESULTS

The ESXD patterns collected on sample *A* (at room temperature) up to 6.7 GPa are shown in Fig. 4. The LiF(111) and BN(100) Bragg peaks of the sample environment are visible in the figure. The appearance of new Bragg peaks, clearly observed above 4.2 GPa, is interpreted as clear evidence for the process of Ga crystallization. In fact, these peaks do not correspond to any interplanar distance of the sample components (BN, LiF). Instead, these Bragg reflections are compatible with the (101) and (002) interplanar distances of the Ga(III) crystalline phase. A tiny feature that can be associated with the Ga(III) (101) reflection is observed also at 2.9 GPa (see Fig. 4). Unfortunately, some data are missing at lower pressures, preventing a clear assignment of the onset of the crystallization. However, the Ga(III) (013) peak, as detected on a different channel, is not observed at 2.3 GPa, as shown in the inset of Fig. 4, and this

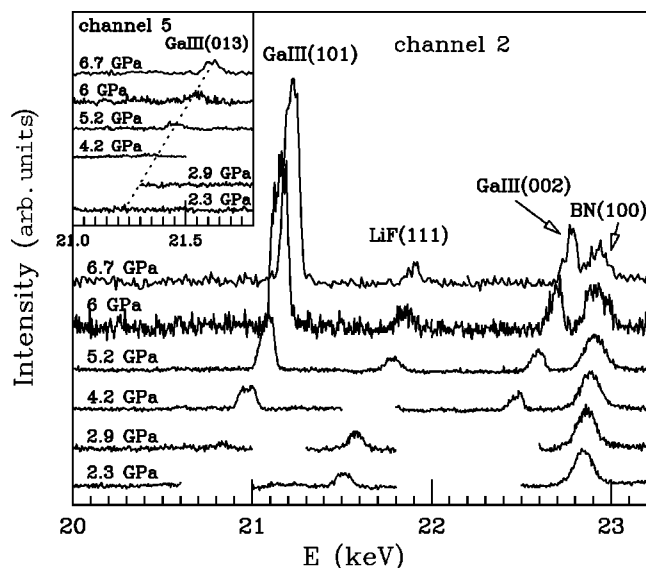


FIG. 4. ESXD patterns of Ga emulsion (sample A) collected at room temperature on channel 2 of the multichannel collimator of the ESXD setup. From the bottom to the top the patterns at 2.9 GPa, 4.2 GPa, 5.2 GPa, 6 GPa, and 6.7 GPa are shown. The ESXD patterns are normalized to the intensity of the BN(100) peak. The trend of the Ga(III) (013) peak, as detected on channel 5 for increasing pressures, is shown in the inset. The dashed line is a linear approximation of the position of the peak at various pressures. The peak is clearly absent below 2.9 GPa.

can be understood in terms of the presence of a metastable liquid. We believe that the intensity of those peaks is not affected by preferred crystal orientation, both because crystal grains nucleate from isolated droplets and because measurements are performed while rotating the cell, as described in Sec. IV. As can be seen in Fig. 4, the intensity of the Ga peaks increases as a function of pressure, showing that a larger number of droplets tends to nucleate, increasing the pressure.

The appearance of Ga(III) in a region where Ga(II) is known to be the stable phase was previously observed in other works by means of x-ray diffraction²⁴ and absorption²⁶ techniques. Previous works^{23,24,26,27} also established the liquid-Ga(II) phase transition (at room temperature) as occurring at about 1.9 GPa. In the present experiment, it is inferred that, similarly to the undercooling experiments at ambient pressure, these liquid Ga droplet ensembles can be overpressurized above the known melting point in a metastable liquid state. The intensity increase of the Ga(III) Bragg peaks with increasing pressure for $P > 2.9$ GPa indicates that crystallization involves only a fraction of droplets and that this fraction increases with pressure. This is not surprising since each droplet is independent from the others, being separated by the epoxy-resin matrix, and will nucleate independently. This means that some droplets can crystallize, while the others remain in the undercooled liquid state.

VI. TEMPERATURE SCANS RESULTS

Recently, it has been emphasized that the shape of the x-ray absorption spectrum near the edge of an absorbing cen-

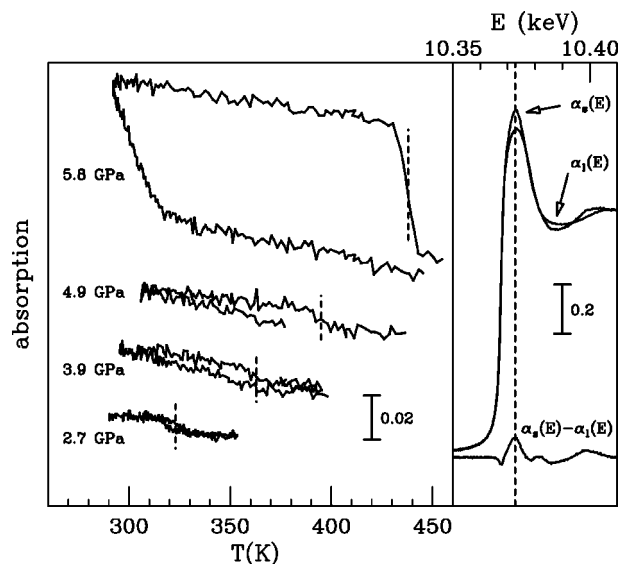


FIG. 5. Left panel: temperature scans of the absorption coefficient at constant energy (SEXAD) at various pressures. The melting temperatures are indicated as vertical dashed lines for each loop, and they are in good agreement with published data.^{23,24,26} Right panel: raw absorption spectra for solid [$\alpha_s(E)$] and liquid [$\alpha_l(E)$] phase and difference spectrum. The maximum contrast-energy point is at $E=10.3727$, as indicated by the dashed line.

ter changes discontinuously when photoabsorbing atoms undergo a phase transition.²⁸ By scanning the temperature at an energy point (SEXAD) of high contrast between two absorption spectra associated with different phases, it is possible to monitor the structural changes occurring in condensed matter. This technique has been previously applied to gallium droplets confined in epoxy resin⁷ with the result of observing a large hysteresis loop with deep undercooling (solidification temperature of about 150 K) and depressed melting temperature $T_m \approx 254$ K, about 50 K below the α -Ga value at ambient conditions.

In Fig. 5 we present the absorption coefficient as a function of temperature at different pressures for sample B, at constant energy $E=10.3727$ keV. This energy gives the maximum contrast between the solid and liquid phase, as shown in the inset of Fig. 5. Temperature scans (SEXAD) were recorded at 2.7 GPa, 3.9 GPa, 4.9 GPa, and 5.8 GPa at the same fixed energy. In Fig. 5 the 5.8 GPa SEXAD presents an evident discontinuity associated with the solid-liquid phase transition. The melting temperature is estimated to be $T_m=438 \pm 5$ K, while the solidification temperature is $T_s=308 \pm 5$ K. At this temperature the sample appears to be solidified as also shown by the EXAFS-fitting results. The shape of the hysteresis loop at 5.8 GPa provides additional evidence that only a single solid phase [i.e., Ga(III)] is observed. No evidence for discontinuities associated with the possible Ga(III)-Ga(II) phase transition (reported in the known phase diagram, Fig. 3) was obtained from the experiment. This is in agreement with previous observations that the liquid nucleates into Ga(III)²⁹ and that transformation to Ga(II) is obtained upon cooling.^{24,30}

The melting temperatures at 2.7 GPa, 3.9 GPa, and 4.9 GPa are estimated to be $T_m=326 \pm 5$ K, $T_m=365 \pm 5$ K,

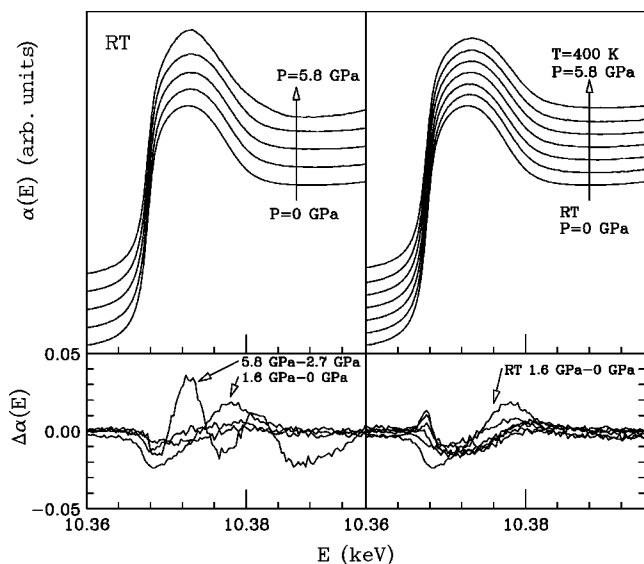


FIG. 6. Upper panels: XAS Ga K -edge spectra of sample B as a function of pressure at room temperature (at ambient pressure, at $P=1.6, 1.9, 2.7$ and 5.8 GPa), on the left, as a function of pressure and temperature, above the melting curve, on the right. Lower panels: difference signals $\Delta\alpha(E)$ of XAS spectra recorded at different pressures and temperatures.

and $T_m=394\pm 5$ K, respectively. The temperature scans at these pressures present quite a smaller discontinuity in comparison with that of 5.8 GPa. This is consistent with the occurrence of a partial-sample crystallization, and it is due to the melting of the minority fraction of the crystallized droplets. We estimated the atomic fraction of crystallized gallium before melting at 2.7 GPa, 3.9 GPa, and 4.9 GPa by comparing the absorption discontinuity at these pressures with that at 5.8 GPa. We assumed that all of the Ga droplets were crystallized above 5.8 GPa, as also indicated by subsequent XAS data analysis (see next section). As a result, at 4.9 -GPa and 3.9 -GPa SEXAD we determined the crystalline Ga-sample fraction to be about 12%, compared with the solid gallium present in the sample at 5.8 GPa and 308 K. The temperature scan at 2.7 GPa instead indicated a partial crystallization involving 9% on the Ga atoms.

VII. XAS DATA ANALYSIS AND RESULTS

A. K -edge shape analysis

High-resolution and low-noise K -edge x-ray absorption near edge-structure spectra were collected as a function of pressure and temperature as reported in Fig. 6 (upper panels). The left-hand-side panel of Fig. 6 shows the spectra recorded at room temperature as a function of pressure. In the right-hand-side panel the spectra refer to the liquid phase, near the melting transition, as a function of pressure. In both panels we report the spectra of undercooled liquid Ga under ambient conditions (300 K, 0 GPa). The lower panels of Fig. 6 report the difference $\Delta\alpha(E)$ between the spectra collected at subsequent pressures to highlight possible changes in the local structure and/or density of unoccupied electronic states.

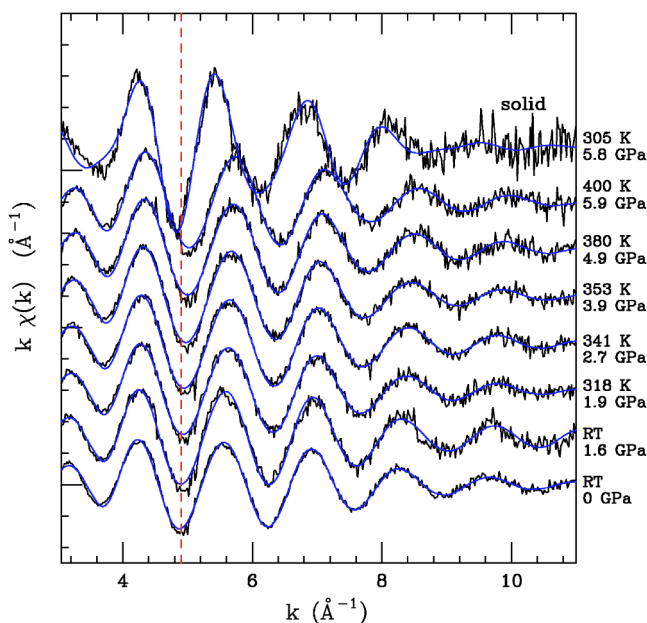


FIG. 7. Experimental $k\chi(k)$ XAS signals compared with the best-fit calculated spectra for liquid and solid (upper signal) Ga. It is reported as a function of the k -wave vector of the photoelectron.

Looking at the difference spectra for increasing pressure (left) at room temperature, a clear change in the absorption is obtained between 5.8 GPa and 2.7 GPa, monitored by the deep minimum at $E=10.3767$ keV, the Ga K edge, and the maximum at $E=10.3729$ keV, the white line, defined as the maximum of x-ray absorption coefficient $\alpha(E)$. The $\Delta\alpha(E)$ curve corresponds to the difference between a solid Ga XAS spectrum and a spectrum related to a sample with a very low percentage of solid gallium (9% in wt) as confirmed by previous SEXAD analyses.

At lower pressures, the $\Delta\alpha(E)$ curves show a change in the local structure between 1.6 GPa and 0 GPa. As shown in figure, the shape of this difference curve is quite different from that obtained between 5.8 GPa and 2.7 GPa, and it is also different from a typical $\Delta\alpha(E)$ curve obtained as a difference between the two liquid Ga XAS spectra (right). If we look at the difference curves in the liquid phase, we do not observe significant variations apart from the difference curve obtained between 1.6 GPa and 0 GPa. This $\Delta\alpha(E)$ curve could be associated with a change in the local structure in the liquid-gallium droplets.

B. EXAFS analysis

Structural variations in the local structure can be visualized by looking at the changes in the shape of the $k\chi(k)$ XAS structural signals. Experimental XAS $k\chi(k)$ signals of liquid Ga as a function of pressure and temperature and solid Ga (upper signal) are presented in Fig. 7. The dashed line at $k=4.9$ \AA^{-1} allows us to highlight the clear changes of the oscillation frequency related to modification of the first-neighbor distances. The sudden variation at 5.8 GPa between 410 K and 305 K related to the liquid-solid phase transition is revealed both by the enhancement of the amplitude and the

increase of the frequency of the XAS spectra. The evident increase of the oscillation amplitude in the $k\chi(k)$ signal is consistent with the enhancement of density after solidification in Ga(III) ($\rho_l = 6.095 \text{ g cm}^{-3} < \rho_{\text{Ga(III)}} = 6.570 \text{ g cm}^{-3}$).

The EXAFS data analysis has been carried out using the GNXAS package.^{31,32} The fitting was performed directly on the absorption data without any noise filtering or preliminary background subtraction. The data analysis of solid Ga, at 5.8 GPa and 305 K, was performed using the local structure of Ga(II) (eight first-neighbor atoms at $\sim 2.78 \text{ \AA}$ and four at about 3.33 \AA) and Ga(III) (four first-neighbor atoms around 2.81 \AA and eight around 2.98 \AA) obtained by Bosio.²⁴

The results of the fitting procedure do not allow us to unambiguously identify the local structure of solid Ga in those pressure and temperature conditions. The experimental signal is compatible with both Ga(III) and Ga(II) structures.

In Fig. 7 the best-fit calculated XAS signals are compared with the experimental data for the liquid and solid phases. The good agreement between the theoretical and experimental signals is evident from the figure.

As regards the XAS data analysis of liquid gallium, the most important contribution to the XAS structural signal is associated with the first-neighbor peak.²⁶ A convenient method to analyze the XAS spectra consists of the decomposition of the $g(r)$ obtained by diffraction experiments or computer simulations into a short-range peak and a long-range tail.³³ The $g(r)$ long-range asymptotic behavior is retained, while the short-range part has to be refined.

In particular, the data analysis of the XAS spectra of liquid gallium has been analyzed, considering the $g(r)$ obtained by x-ray diffraction [$g(r)$ model].³⁴ The radial distribution function $p(r)$ [RDF, $p(r) = 4\pi r^2 \rho g(r)$] has been reconstructed for liquid gallium starting from the structural parameters determined by the XAS data analysis. Previous x-ray diffraction measurements³⁵ on liquid gallium showed that the position of the maximum of the radial distribution function $p(r)$ slightly decreases upon increasing pressure. Very recently,²⁶ the reconstruction of $g(r)$ starting from the XAS data analysis on liquid gallium confirmed this result. It was also observed that the height of the first-neighbor peak in liquid gallium slightly increased with pressure (at $T=298 \text{ K}$, 378 K , and 498 K). By increasing the temperature, at constant pressure, the maximum of the $g(r)$ function moved toward shorter distances, while the height of the first-neighbor peak dramatically decreased. This strong dependence on temperature was also previously observed by neutron diffraction measurement at ambient pressure.³⁶

In Fig. 8 we report the radial distribution function $p(r)$ calculated by the XAS data results for liquid gallium as a function of pressure and temperature. The local, average structure of liquid gallium at room temperature and ambient pressure (dashed line) is compatible with that of liquid gallium at ordinary pressure, measured by neutron³⁶ and x-ray³⁴ diffraction. Looking at Fig. 8, it is evident that by increasing the pressure and temperature the height of the first-neighbor peak of $p(r)$ decreases, while the position of the maximum of the function moves toward shorter distances, as shown by the arrow reported in the figure. This trend confirms the previous studies showing the $p(r)$ dependence on both pressure and

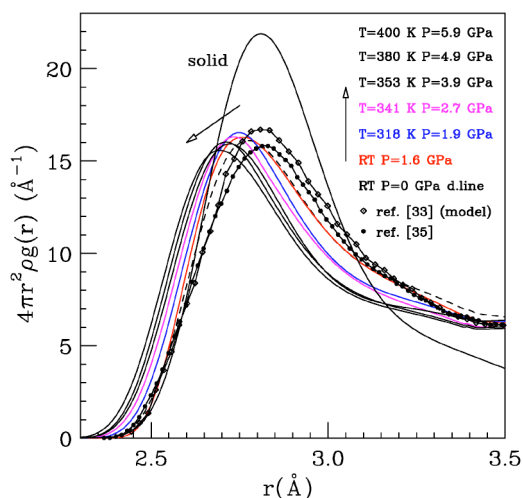


FIG. 8. (Color online) Radial distribution function $p(r)$ for solid gallium and for liquid gallium as a function of temperature and pressure. The RDF reconstructed by the neutron³⁶ and x-ray diffraction data (model)³⁴ are also reported for comparison. The arrow shows the $p(r)$ trend for increasing pressure and temperature.

temperature. The position of the maximum of RDF is gradually shifted toward shorter distances from 2.77 \AA (at room temperature and ambient pressure) to 2.69 \AA (at 400 K and 5.8 GPa). The $p(r)$ peak intensity, with the increase of pressure and temperature, decreases from 16.5 \AA^{-1} (at 318 K and 1.9 GPa) to 15.6 \AA^{-1} (at 400 K and 5.8 GPa).

The changes in the distance and height of the first peak correspond to the frequency and amplitude variations in the original XAS signals (Fig. 7). In the case of solid gallium $p(r)$, the first-neighbor peak is dramatically shifted to longer distances and its intensity increases, as confirmed by the XAS signal reported in Fig. 7.

The XAS data analysis of measurements related to the sample in the condition of *partial crystallization* (at room temperature and 2.7 GPa, at 330 K and 3.9 GPa, and at 340 K and 5.8 GPa, see also Fig. 3) has been carried out by introducing in the fitting procedure for liquid gallium also a solid component, firstly of the Ga(II) structure and then of Ga(III) solid phase. We have considered only the first and the third shells of the Ga(II) structure (eight first-neighbor atoms at 2.78 \AA and eight at 4.07 \AA), because the contribution to the total signal of the second shell (four first-neighbor atoms) is less important. For the Ga(III) component we introduced the first and the second shell (four first-neighbor atoms around 2.81 \AA and eight around 2.98 \AA).

The intensity of the $k\chi(k)$ XAS signals related to the solid component was weighted by taking into account the fraction of crystallized gallium estimated from the SEXAD analysis reported above.

The XAS data analysis for Ga under these pressure and temperature conditions was carried out also without considering the solid component. Any difference in the residual curve obtained from the three models [liquid, liquid+Ga(II), and liquid+Ga(III)] has been shown by the fitting procedure. The quantity of solid gallium is insufficient to obtain significant fitting results of the solid component.

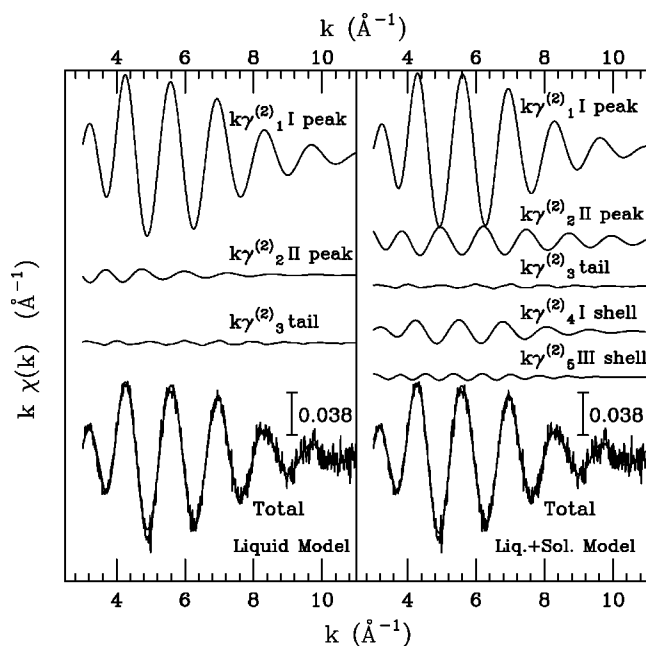


FIG. 9. Pair contributions $k\chi(k)^{(2)}$ associated with the two first-neighbor shells, describing the first $g(r)$ peak and the long-range tail (on the right), pair contributions $k\chi(k)^{(2)}$ associated with the first $g(r)$ peak and the long-range tail and those associated with the first and the third coordination shells of Ga(II). The total $k\chi(k)$ signal calculated by the liquid and liquid+solid model is compared with the experimental spectrum of liquid gallium at room temperature and 2.7 GPa. It is evident that both models are compatible with the experimental signal.

In Fig. 9 we present the comparison between the theoretical and experimental $k\chi(k)$ signal at room temperature and 2.7 GPa. The theoretical signal has been calculated both by considering a part of the solid component of Ga(II) (on the left) and starting from a purely liquid model (on the right). It is evident that both models are compatible with the experimental signal.

VIII. CONCLUSIONS

In this work we studied phase transitions and local structure on fully characterized samples composed of micrometric droplets of liquid gallium under pressure, using advanced x-ray techniques such as EXAFS, SEXAD, and ESXD.

Measurements were performed in a broad range of pressures and temperatures (0–6.7 GPa and 298–440 K). We provided evidence that, in the high-pressure range, liquid Ga can be actually overpressurized into a metastable liquid state

for a sufficient time to perform x-ray diffraction and spectroscopy measurements aimed at determining the nature of the structure and electronic properties of this metastable state. This is similar to what previous experiments performed at ambient pressure have shown, starting from the results of Turnbull and Cech^{1–3} and including the more recent studies about the undercooling capabilities of samples consisting of a dispersion of micrometric droplets,^{7,12,13,37} but, in addition, the present experiment encourages the full investigation of the role of the pressure variable.

The ESXD patterns and the SEXAD analysis show that the quantity of crystalline Ga increases as a function of pressure. A large fraction of the droplets of our emulsions are still liquid at high pressure, in a region where Ga is known to be crystalline. In particular, ESXD patterns collected at room temperature as a function of pressure show the appearance of detectable Ga(III) Bragg peaks above 4.2 GPa, assessing the metastability of the liquid phase in the wide-pressure range. However, a very low quantity of crystalline Ga was observed at 2.9 GPa. Traces of crystallization involving a limited portion of droplets were found at 2.7 GPa by SEXAD analysis, while crystallization was clearly observed at 5.8 GPa. Slight differences in the crystallization properties probed by ESXD and SEXAD can be assigned to the thermodynamic paths of the samples.

The radial distribution function $p(r)$ of liquid Ga was reconstructed as a function of pressure and temperature above the melting curve. The maximum of the first $p(r)$ peak is slightly shifted toward short distances and its height decreases with increasing temperature and pressure. The local, average structure of liquid gallium at room temperature and ambient pressure is compatible with that obtained at ordinary pressure, measured by diffraction techniques.^{34,36}

The subtle differences in the x-ray absorption spectra of liquid Ga, especially in the K -edge region, monitored by $\Delta\alpha(E)$ curves (see Fig. 6), may indicate that some transformations involving microscopic structure and/or electronic states occur for this system in the 0–2-GPa region of the phase diagram at room temperature. The exciting hypothesis that this observation is related to a liquid-liquid phase transition occurring in the undercooled liquid region, which at present should be regarded as a speculation, stimulates further detailed investigations on this system.

ACKNOWLEDGMENTS

R. P. thanks the Istituto Nazionale per la Fisica della Materia (INFN) and the ESRF for the financial support during her stay at the ESRF.

¹D. Turnbull and R. E. Cech, J. Appl. Phys. **21**, 804 (1950).

²D. Turnbull, J. Appl. Phys. **21**, 1022 (1950).

³D. Turnbull, J. Chem. Phys. **20**, 411 (1952).

⁴Y. Miyazawa and G. M. Pound, J. Cryst. Growth **23**, 45 (1974).

⁵L. Bosio and C. G. Windsor, Phys. Rev. Lett. **35**, 1652 (1975).

⁶S.-F. Tsay and S. Wang, Phys. Rev. B **50**, 108 (1994).

⁷A. Di Cicco, Phys. Rev. Lett. **81**, 2942 (1998).

⁸J. N. Glosli and F. H. Ree., Phys. Rev. Lett. **82**, 4659 (1999).

⁹I. Saika-Voivod, F. Sciortino, and P. H. Poole, Phys. Rev. E **63**, 011202 (2001).

- ¹⁰G. Franzese, G. Malescio, A. Skibinsky, S. V. Buldyrev, and H. E. Stanley, *Nature (London)* **409**, 692 (2001).
- ¹¹A. Filippini, *J. Phys.: Condens. Matter* **13**, R23 (2001).
- ¹²L. Ottaviano, A. Filippini, and A. Di Cicco, *Phys. Rev. B* **49**, 11 749 (1994).
- ¹³A. Di Cicco, S. Fusari, and S. Stizza, *Philos. Mag. B* **79**, 2113 (1999).
- ¹⁴A. Filippini, M. Borowski, D. T. Bowron, S. Ansell, A. Di Cicco, S. De Panfilis, and J.-P. Itiè, *Rev. Sci. Instrum.* **71**, 2422 (2000).
- ¹⁵A. Filippini, V. M. Giordano, S. D. Panfilis, A. Di Cicco, E. Principi, A. Trapananti, M. Borowski, and J.-P. Itiè, *Rev. Sci. Instrum.* **74**, 2654 (2003).
- ¹⁶J. M. Besson, R. J. Nelmes, G. Hamel, J. S. Loveday, G. Weill, and S. Hull, *Physica B* **180&181**, 907 (1992).
- ¹⁷P. Vinet, J. R. Smith, J. Ferrante, and J. H. Rose, *Phys. Rev. B* **35**, 1945 (1987).
- ¹⁸P. Vinet, J. Ferrante, J. R. Smith, and J. H. Rose, *J. Phys. C* **19**, L467 (1986).
- ¹⁹R. W. Roberts and C. S. Smith, *J. Phys. Chem. Solids* **31**, 619 (1970); **31**, 2397 (1970).
- ²⁰K. O. McLean and C. S. Smith, *J. Phys. Chem. Solids* **33**, 279 (1972).
- ²¹C. S. Smith and L. S. Cain, *J. Phys. Chem. Solids* **36**, 205 (1975).
- ²²G. R. Barsch and Z. P. Chang, *Accurate Characterization of the High-Pressure Environment*, edited by E. C. Lloyd (Washington D.C.: US Government Printing Office) 326, 173 (1971).
- ²³A. Jayaraman, W. K. Jr., and G. C. Kennedy, *Phys. Rev.* **130**, 540 (1963).
- ²⁴L. Bosio, *J. Chem. Phys.* **68**, 1222 (1978).
- ²⁵O. Schulte and W. B. Holzapfel, *Phys. Rev. B* **55**, 8122 (1997).
- ²⁶L. Comez, A. Di Cicco, J.-P. Itiè, and A. Polian, *Phys. Rev. B* **65**, 014114 (2002).
- ²⁷O. Degtyareva, M. I. McMahon, D. R. Allan, and R. J. Nelmes, *Phys. Rev. Lett.* **93**, 205502 (2004).
- ²⁸A. Filippini, M. Borowski, P. W. Loeffen, S. De Panfilis, A. Di Cicco, F. Sperandini, M. Minicucci, and M. Giorgetti, *J. Phys.: Condens. Matter* **10**, 235 (1998).
- ²⁹E. Weir, G. J. Piermarini, and S. Block, *J. Chem. Phys.* **54**, 2768 (1971).
- ³⁰L. Bosio, *C.R. Seances Acad. Sci., Ser. A* **270**, 1453 (1970).
- ³¹A. Filippini, A. Di Cicco, and C. R. Natoli, *Phys. Rev. B* **52**, 15 122 (1995).
- ³²A. Filippini and A. Di Cicco, *Phys. Rev. B* **52**, 15 135 (1995).
- ³³A. Filippini, *J. Phys.: Condens. Matter* **6**, 8415 (1994).
- ³⁴A. H. Narten, *J. Chem. Phys.* **56**, 1185 (1972).
- ³⁵K. Tsuji, *J. Non-Cryst. Solids* **27**, 117 (1990).
- ³⁶M. C. Bellissent-Funel, P. Chieux, D. Levesque, and J. J. Weis, *Phys. Rev. A* **39**, 6310 (1989).
- ³⁷A. Di Cicco and A. Filippini, *Europhys. Lett.* **27**, 407 (1994).